SPECIALISTS MEETING ON SMALL BREAK LOCA ANALYSES IN LWRs

Pisa, Italy, 23 – 27 June 1985

organized by

Dipartimento di Costruzioni Meccaniche e Nucleari
Università di Pisa

in cooperation with

ENEA, IAEA, NEA, NRC

with the sponsorship of

ANDIN, ANS, EEC, ENS, SNI

OFFPRINT

GIARDINI EDITORI
E STAMPATORI
IN PISA

NON EQUILIBRIUM MODELING OF TWO-PHASE CRITICAL FLOW IN PIPES AND JET EXPANSION REGION

Flavio Dobran

Stevens Institute of Technology
Hoboken, New Jersey, 07030, U.S.A.

ABSTRACT

The results of nonequilibrium modeling of the two-phase critical flow in tubes and in the jet expansion region are presented as a function of the stagnation pressure and subcooling of liquid in the vessel to which the tube is attached and of the geometric characteristics of the tube such as its length and diameter. The two-phase flow modeling involves the use of the basic conservation and balance equations of each phase which were numerically solved to obtain the critical flow at the tube end and the steady state axisymmetric flow distribution in the jet. The numerical results are compared with the experimental data of critical flow rates and pressure distributions in tubes and with the total pressure distribution in the jet at various locations along the jet. In both of these situations it is shown that this comparison is very good and that the numerical models can be used to study the jet forces.

1. INTRODUCTION

The two-phase critical flow discharge through tubes and the development of flow in the jet expansion region on the outside of the tube play important roles in the safety design of nuclear reactors. The critical flow rate in a tube may occur during the tube rupture in a pressurized water reactor carrying a high pressure liquid coolant and as such it depends on the state of the fluid on the upstream of the break and on the characteristics of the break itself. As the fluid expands in the tube, from a high pressure in the vessel to which the tube is attached to the low pressure of the atmosphere on the outside of the tube, it flashes into a two-phase mixture. This mixture may then produce significant forces from its expanding jet on the outside of the tube on the equipment that may be located in the path of the high velocity two-phase jet.

1.1 Previous Work and Objectives of the Paper

Many studies have been carried out in the past on the two-phase critical flows in tubes and the reviews of these may be found in [1-5]. These studies were concerned with the homogeneous or equilibrium models and with a wide variety of the nonequilibrium models. The equilibrium models assume the equality of phase temperatures, pressures and flow velocities and are found to model the two-phase critical flows well whenever the residence time of a fluid particle in the tube is large and the subcooling of the liquid in the vessel to which the tube is attached is small. For short tubes and subcooled liquid conditions, the equilibrium modeling of two-phase critical flows is not adequate and a recourse to the nonequilibrium modeling is necessary for the proper prediction of critical flow parameters.

The nonequilibrium modeling assumes hydrodynamic and thermal nonequilibrium between the phases. Although a wide variety of such models have been considered over the years [1-4], the best modeling approaches have proved to be those which are based on the separate conservation and balance equations of each phase, so that the critical flow at the tube end is determined on the basis of the history of flow up to the critical point. The detailed two-phase flow modeling also requires the specification of constitutive equations as a function of the flow regime which may not be known sufficiently well and, therefore, this modeling approach may not be very desirable in some situations.

When a two-phase mixture exits from a tube with the critical or maximum flow rate, the mixture readily expands into the ambient atmosphere due to the considerable pressure differential that may exist between the fluid at the tube exit and the atmosphere. This pressure difference produces different rates of expansion of the liquid and gas phases and may lead to considerable nonequilibrium between the phases in the two-phase jet expansion region. Consequently, an equilibrium two-phase flow modeling in the jet is not expected to be reasonable and the flow conditions at the tube exit may significantly affect the flow evolution in the jet.

From the above it is clear that the two-phase flow modeling of the jet should involve hydrodynamic and thermal nonequilibrium and that the flow conditions at the tube exit should be also determined by a nonequilibrium critical flow model in order to predict the jet flow characteristics reliably as a function of tube geometric characteristics and liquid

stagnation conditions. The objectives of this paper are, therefore, the following: (1) to present nonequilibrium models for modeling the critical flows in tubes and flows in the jet expansion region, (2) to compare the model predictions with the experimental data, and (3) to discuss the numerical results pertaining to the flow distribution.

2. TWO-PHASE FLOW MODELING

To model the two-phase critical flow in a tube and flow in the jet expansion region use will be made of the one- and two-dimensional form of the conservation and balance equations of two-phase flow, respectively. During the two-phase critical flow discharge through a tube, the disturbances in the jet cannot propagate upstream into the tube and it is permissible to solve separately the critical flow in the tube and then to use the fluid conditions at the tube exit as the boundary conditions for a model of the flow in the jet. This approach will be followed here for the interest of simplicity in the overall modeling and also for the purpose of developing separate modeling capabilities in each flow region.

2.1 Two-Phase Critical Flow Modeling

The critical flow in tubes will be modeled by a set of nonequilibrium two-phase flow equations assuming a steady state and one-dimensional flow. For the purpose of some simplicity in the model, it is also assumed that the gas phase is thermal equilibrium (at a local saturation pressure) and that both phases are at the same pressure at any cross-section of the duct. From the conservation of mass equations of gas and liquid,

$$M_G = \alpha \rho_G A u_G = xM \tag{2.1}$$

$$M_L = (1-\alpha)\rho_L A u_L = (1-x)M \tag{2.2}$$

and equations of state

$$\rho_G = \rho_G(P) \tag{2.3}$$

$$\rho_L = \rho_L(h_L, P) \tag{2.4}$$

where M denotes the mass flow rate, x the quality, α the gas volumetric or void fration, A the cross-sectional area of the tube, u the velocity along the axis of the tube, ρ the density, P the pressure and h the enthalpy. The subscripts G and L denote the gas and liquid phases. With z denoting the axial distance along the tube, the governing conservation and balance equations of two-phase flow may be written in the following form [5]:

$$\rho_G A u_G \frac{d\alpha}{dz} + \alpha A u_G \frac{d\rho_G}{dP}\frac{dP}{dz} + \alpha \rho_G A \frac{du_G}{dz} - M\frac{dx}{dz} = -\alpha \rho_G u_G \frac{dA}{dz} \tag{2.5}$$

$$-\rho_L A u_L \frac{d\alpha}{dz} + (1-\alpha)A u_L \left(\frac{\partial \rho_L}{\partial P}\right)_{h_L}\frac{dP}{dz} + (1-\alpha)\rho_L A \frac{du_L}{dz} + M\frac{dx}{dz} + (1-\alpha)A u_L \left(\frac{\partial \rho_L}{\partial h_L}\right)_P \frac{dh_L}{dz} = -(1-\alpha)\rho_L u_L \frac{dA}{dz} \tag{2.6}$$

$$\alpha \rho_G A u_G \frac{du_G}{dz} = -\alpha A \frac{dP}{dz} - F_{LG}A - F_{WG}A - \eta(u_G - u_L)M\frac{d\alpha}{dz} - \rho_G g \alpha A \cos\theta \tag{2.7}$$

$$(1-\alpha)\rho_L A u_L \frac{du_L}{dz} = -(1-\alpha)A\frac{dP}{dz} + F_{LG}A - F_{wL}A - (1-\eta)(u_G-u_L)M\frac{dx}{dz} - \rho_L g(1-\alpha)A\cos\theta \quad (2.8)$$

$$M[h_{LG} + \frac{1}{2}(u_G^2-u_L^2)]\frac{dx}{dz} + [xM\frac{dh_G}{dP}]\frac{dP}{dz} + [xMu_G]\frac{du_G}{dz} + [(1-x)Mu_L]\frac{du_L}{dz} + [(1-x)M]\frac{dh_L}{dz} + Mg\cos\theta = 0 \quad (2.9)$$

$$M[h_{LG} + \frac{1}{2}(u_G^2-u_L^2)]\frac{dx}{dz} = \frac{dQ_L}{dz} \quad (2.10)$$

Equations (2.5) and (2.6) above represent the conservation of mass of gas and liquid, (2.7) and (2.8) are the momentum and (2.9) and (2.10) are the energy balance equations of the two phases. In the momentum equations F_{LG} is the drag force per unit volume acting on the liquid phase in the direction of flow, and in the opposite direction on the gas phase, F_{wG} and F_{wL} are the drag forces per unit volume exerted by the tube wall on the gas and liquid, respectively, and θ=90° for horizontal flow and 0° for vertical upflow. In the energy equations (2.9) and (2.10) η represents the effect of phase change and it may be assumed to be equal to 1/2 [6], h_{LG} is the enthalpy of evaporation and dQ_L/dz denotes the heat transfer rate per unit tube length from the liquid to the gas. For bubbly and separated flows with liquid adjacent to the tube wall, it may be assumed that F_{wG}=0, whereas the interphase drag force F_{LG} may be modeled as follows:

$$F_{LG} = \xi_{GG}(u_G-u_L) + \Delta_{GG}(u_G\frac{du_G}{dz} - u_L\frac{du_L}{dz}) \quad (2.11)$$

where $\xi_{GG}\geq 0$ is the viscous drag coefficient and $\Delta_{GG}\geq 0$ is the virtual mass coefficient which accounts for the relative acceleration between the phases [5].

Equations (2.5)-(2.10) can be solved for the 6 unknowns: α, x, u_G, u_L, P and h_L provided that the constitutive equations are supplied for ξ_{GG}, Δ_{GG}, F_{wL} and dQ_L/dz. The tube cross-sectional area is assumed to be given and the mass flow rate is treated as a parameter. The thermodynamic properties are specified through $h_G(P)$, $\rho_G(P)$ and $\rho_L(h_L,P)$ which are also assumed to be given.

Constitutive Equations. The constitutive equations for the interfacial drag, virtual mass, wall friction and interphase transfer rate are specified according to the flow regime which varies along the tube. Close to the tube entrance the flow is bubbly, but further downstream it may revert to the churn-turbulent and annular flow patterns at higher void fractions. The constitutive equations for ξ_{GG}, Δ_{GG}, F_{wL} and dQ_L/dz account for such a flow regime change on the basis of the void fraction and are discussed in detail in [5] and may be also found in [4,6-8].

Initial Conditions. The solution of the ordinary differential equations [2.5-2.10] requires the specification of initial conditions. The fluid in the vessel at z=0 is assumed to be at stagnation conditions characterized by

stagnation pressure and subcooling. Based on this information, tube inlet geometry and diameter and the liquid superheat required for the onset of bubble nucleation [9], it is possible to find the position along the tube where two-phase flow occurs and to use this information to find initial conditions for the two-phase flow model [5].

Solution Procedure. Equations [2.5-2.10] may be written in the following form:

$$A^*\frac{dX}{dz} = B^* \quad (2.12)$$

where $X=(\alpha, x, u_G, u_L, P, h_L)^T$ is the vector of dependent variables and A^* and B^* are matrices which depend on X. With the initial conditions discussed above, (2.12) can be solved in terms of the stagnation conditions of liquid in the vessel (pressure and subcooling) and tube geometric characteristics (tube diameter and length) for the critical flow rate at the tube exit which is determined by the following set of sufficient and necessary conditions [10]:

$$\Delta=0 \text{ and } n_i=0,\ i=1,\ldots,6 \quad (2.13)$$

where $\Delta=\det(A^*)$ is the determinant of A^* and n_i is the determinant obtained by replacing the i^{th} column of A^* by the column vector B^*. The solution of these equations was performed by a variable step Runge-Kutta method described in [5] and the critical flow results are discussed below.

2.2 Two-Phase Flow Jet Modeling

The axisymmetric jet configuration is characterized by the radial coordinate r and the axial coordinate z with the radial and axial velocities denoted by v and u, respectively. The velocity vector is denoted by U and the time by t. With these notations, the modeling of the two-dimensional and two-phase flow jet with phase change may be performed by the following system of nonequilibrium two-phase flow equations [11-13]:

$$\frac{\partial r^n f}{\partial t} + \frac{\partial r^n F}{\partial z} + \frac{\partial r^n G}{\partial r} = S \quad (2.14)$$

where f is the vector of dependent variables and F, G and S are the vectors which depend on f, i.e.

$$f = \begin{bmatrix} \bar{\rho}_L \\ \bar{\rho}_G \\ \bar{\rho}_L u_L \\ \bar{\rho}_L v_L \\ \bar{\rho}_G u_G \\ \bar{\rho}_G v_G \\ \bar{\rho}_L[\varepsilon_L + (u_L^2 + v_L^2)/2] \\ \bar{\rho}_G[\varepsilon_G + (u_G^2 + v_G^2)/2] \end{bmatrix} \quad (2.15)$$

$$F = \begin{bmatrix} \bar{\rho}_L u_L \\ \bar{\rho}_G u_G \\ (\bar{\rho}_L u_L)^2/\bar{\rho}_L + (1-\alpha)P \\ (\bar{\rho}_L u_L)(\bar{\rho}_L v_L)/\bar{\rho}_L \\ (\bar{\rho}_G u_G)^2/\bar{\rho}_G + \alpha P \\ (\bar{\rho}_G u_G)(\bar{\rho}_G v_G)/\bar{\rho}_G \\ (\bar{\rho}_L u_L)[\varepsilon_L + (u_L^2+v_L^2)/2 + (1-\alpha)P/\bar{\rho}_L] \\ (\bar{\rho}_G u_G)[\varepsilon_G + (u_G^2+v_G^2)/2 + \alpha P/\bar{\rho}_G] \end{bmatrix} \qquad (2.16)$$

$$G = \begin{bmatrix} \bar{\rho}_L v_L \\ \bar{\rho}_G v_G \\ (\bar{\rho}_L u_L)(\bar{\rho}_L v_L)/\bar{\rho}_L \\ (\bar{\rho}_L v_L)^2/\bar{\rho}_L + (1-\alpha)P \\ (\bar{\rho}_G u_G)(\bar{\rho}_G v_G)/\bar{\rho}_G \\ (\bar{\rho}_G v_G)^2/\bar{\rho}_G + \alpha P \\ (\bar{\rho}_L v_L)[\varepsilon_L + (u_L^2+v_L^2)/2 + (1-\alpha)P/\bar{\rho}_L] \\ (\bar{\rho}_G v_G)[\varepsilon_G + (u_G^2+v_G^2)/2 + \alpha P/\bar{\rho}_G] \end{bmatrix} \qquad (2.17)$$

$$S = \begin{bmatrix} r^n(\Gamma_c-\Gamma_e) \\ r^n(\Gamma_e-\Gamma_c) \\ r^n[\Gamma_c u_G - \Gamma_e u_L + K(u_G-u_L)] \\ r^n[\Gamma_c v_G - \Gamma_e v_L + K(v_G-v_L)] + n(1-\alpha)P \\ r^n[-\Gamma_c u_G + \Gamma_e u_L - K(u_G-u_L)] \\ r^n[-\Gamma_c v_G + \Gamma_e v_L - K(v_G-v_L)] + n\alpha P \\ r^n\{-P\partial(1-\alpha)/\partial t + (1-\alpha)[K + (\Gamma_c+\Gamma_e)/2][(u_L-u_G)^2 + \\ \quad (v_L-v_G)^2] + (\Gamma_c-\Gamma_e)(\varepsilon_G+P/\rho_G) + R(T_G-T_L) - \\ \quad \Gamma_e(u_L^2+v_L^2)/2 + \Gamma_c[u_L(u_G-u_L/2) + \\ \quad v_L(v_G-v_L/2) + K[u_L(u_G-u_L) + v_L(v_G-v_L)] - \\ \quad PU_L.\nabla(1-\alpha)\} \\ r^n\{-P\partial\alpha/\partial t + \alpha[K + (\Gamma_c+\Gamma_e)/2][(u_L-u_G)^2 + \\ \quad (v_L-v_G)^2] - (\Gamma_c-\Gamma_e)(\varepsilon_G+P/\rho_G) - R(T_G-T_L) - \\ \quad \Gamma_c(u_G^2+v_G^2)/2 + \Gamma_e[u_G(u_L-u_G/2) + v_G(v_L-v_G/2)] - \\ \quad K[u_G(u_G-u_L) + v_G(v_G-v_L)] - PU_G.\nabla\alpha\} \end{bmatrix} \qquad (2.18)$$

The above equations are valid at the jet axis where n=0 and away from the axis where n=1. At the axis of the jet $v_G=v_L=0$ and $\partial G/\partial r=0$. The other variables appearing in the above equations are: ε is the internal energy, P is the pressure which is assumed to be the same for the gas and liquid phases, K is the interfacial drag function, Γ_c and Γ_e denote the condensation and evaporation rates, and R is the interfacial heat transfer coefficient. K, Γ_c, Γ_e and R have to be specified by the constitutive equations as discussed below. The partial densities of gas and liquid are defined as:

$$\bar{\rho}_G = \alpha\rho_G \qquad (2.19)$$

$$\bar{\rho}_L = (1-\alpha)\rho_L \qquad (2.20)$$

whereas the equations of state are assumed to be given in terms of pressure and internal energy, i.e.

$$\rho_G = \rho_G(P,\varepsilon_G) \qquad (2.21)$$

$$\rho_L = \rho_L(P,\varepsilon_L) \qquad (2.22)$$

Equations (2.14), after being supplemented by the constitutive equations, allow for the solution of the gas-liquid flow characteristics of the jet. In particular, the pressure can be found by eliminating the void fraction between (2.19) and (2.20), i.e.

$$\bar{\rho}_L\ \rho_L(P,\varepsilon_L) + \bar{\rho}_G\ \rho_G(P,\varepsilon_G) = \rho_L(P,\varepsilon_L)\ \rho_G(P,\varepsilon_G) \qquad (2.23)$$

Constitutive Equations. The constitutive equation for the interfacial drag K is assumed to be a constant and equal to 10^5 Kg/m^2-s, whereas the evaporation and condensation rates are specified by the following equations [11]:

$$\Gamma_e = \lambda_e A(1-\alpha)\rho_L\alpha(T_s R_u)^{1/2}(T_L-T_s)/T_s, \text{ for } T_L \geq T_s$$
$$= 0, \text{ otherwise} \qquad (2.24)$$

$$\Gamma_c = \lambda_c A\alpha\rho_G(1-\alpha)(T_s R_u)^{1/2}(T_s-T_G)/T_s, \text{ for } T_G \leq T_s$$
$$= 0, \text{ otherwise} \qquad (2.25)$$

where A is the interfacial area per unit volume of the mixture and λ_e and λ_c are the time relaxation parameters for evaporation and condensation and are assumed to be equal to 0.1/sec. For N equal size spherical droplets of radius r_p per unit volume and assumed to be equal to 10^{10} m^{-3} and constant, A is given by the following expressions:

$$A = \begin{cases} \alpha^{2/3}(4\pi N/3)^{1/3}, & \text{when } \alpha \leq 0.5 \\ (1-\alpha)^{2/3}(4\pi N/3)^{1/3}, & \text{when } \alpha > 0.5 \end{cases} \quad (2.26)$$

$$r_p = \begin{cases} [3\alpha/4\pi N]^{1/3}, & \text{when } \alpha \leq 0.5 \\ [3(1-\alpha)/4\pi N]^{1/3}, & \text{when } \alpha > 0.5 \end{cases} \quad (2.27)$$

The interfacial heat transfer is modeled as follows:

$$R = \alpha R_G + (1-\alpha)R_L \quad (2.28)$$

where

$$R_G = (1 + 0.37\ Re^{1/2}\ Pr_G^{0.35})/r_p \quad (2.29)$$

$$R_L = 8.067\ k_L/r_p \quad (2.30)$$

$$Pr_G = \mu_G Cp_G/k_G \quad (2.31)$$

$$Re = 2r_p\rho_G|U_G-U_L|/\mu_G \quad (2.32)$$

and T is the temperature, R_μ is the gas constant, k is the thermal conductivity, μ is the viscosity and Cp is the specific heat at constant pressure.

Initial Conditions. The solution of the transient system of differential equations (2.14) requires the specification of initial conditions of the air atmosphere which, for the purpose of keeping the modeling simple, is modeled by a steam atmosphere with the following characteristics: 1) $T_L=T_G=294°K$, 2) P=0.1Mpa, 3) $\alpha=0.999$, 4) $\rho_L=935\ Kg/m^3$, 5) $\rho_G=0.63\ Kg/m^3$, and 6) $U_L=U_G=0$.

Boundary Conditions. The boundary conditions are specified on the edges of the computational domain of the jet. For this purpose, the radial and axial dimensions R_{max} and Z_{max} of the domain should be chosen sufficiently large such that the flow properties in the jet vary significantly only inside this domain. At the exit of the pipe, the gas-liquid properties are determined by the critical flow model as discussed above, while at the outflow boundary at $z=Z_{max}$ it is assumed that the flow properties can be extrapolated from the upstream by a second order accurate extrapolation procedure [14]. The side boundary at $r=R_{max}$ is assumed to be at the initial conditions, except for the radial components of the gas and liquid velocities which are set equal to the corresponding values at one radial node away towards the jet axis. At the inflow boundary at z=0, but excluding the region at the tube end, all properties are set equal to the initial conditions, except for the axial components of gas and liquid velocities which are set equal to the corresponding values at one node downstream in the computational domain at each radial position in the jet.

Solution Procedure. The solution of the system of equations (2.14) was accomplished by the Lax's [11,14] finite difference scheme extended to the two-dimensional flow. The time derivative $\partial\alpha/\partial t$ in the source terms S_7 and S_8 in (2.18) was eliminated by the aid of the liquid continuity equation

with the constant liquid density and all space derivatives in the source terms were then centrally differenced. The numerical procedure constructed in this way proved to be stable with the spatial and time step limitations expressed by the Courant-Friedrichs-Lewy stability condition [14]. The computational domain involved R_{max}=0.16m and Z_{max}=0.35m, where the radial node separation varied from Δr=1.56mm close to the jet axis to Δr=12.5mm close to $r=R_{max}$. The axial node spacings varied from Δz=3.12mm close to the pipe exit to Δz=12.5mm close to $z=Z_{max}$.

Computations were carried out with the initial and boundary conditions discussed above until the steady state jet profile was established. Due to the very high momentum of the two-phase mixture at the pipe exit, the jet profile was established in a few milliseconds.

3. RESULTS AND DISCUSSION

The results obtained by the critical two-phase flow model are depicted in Figs. 1 and 2. Figure 1 illustrates a comparison between the predicted critical mass fluxes through tubes and the steam-water experimental data [5,15] for saturated and subcooled liquid conditions in the vessel and for tube length to diameter ratios up to 300. The stagnation pressure varied from 1-3 MPa. As can be seen from this figure, the predicted critical mass fluxes G_o are within ±10% of the experimental data.

A comparison of the predicted pressure distribution along the tube with the experimental data is illustrated in Fig. 2 for the saturated liquid in the vessel. This and other comparisons presented in [5,15] for a wide range of liquid subcoolings and stagnation pressures and tube length to diameter ratios shows that the proposed two-phase critical flow model is able to reproduce the critical flow discharge well and that the detailed flow conditions at the tube exit (liquid and gas velocities, quality, void fraction and pressure) may be used with confidence as an input to a model of the two-phase flow in the jet.

Using the boundary conditions at the tube exit as an input to the jet model, Figs. 3 and 4 depict the predicted total pressure distribution at different axial positions along the jet and the comparison with the steam-water experimental data [16]. In these figures z/D denotes the ratio of the distance along the jet axis from the tube exit to the tube diameter, while the total pressure in the jet is defined as follows:

$$P_{TOT} = P + 0.5[\alpha\rho_G u_G + (1-\alpha)\rho_L u_L]^2/[\alpha\rho_G + (1-\alpha)\rho_L] \quad (3.1)$$

Figure 3 illustrates the total pressure distribution for the saturated liquid in the vessel, whereas Fig. 4 depicts the distribution for the subcooled liquid with the subcooling of 22°C. The predicted total pressure distribution also compares well with the experiments and it is shown to exibit a double pressure peak.

The occurrence of the double pressure peaks in the jet can be associated with the gas-liquid nonequilibrium flow which may be justified by examining the numerical results of the void fraction and gas and liquid radial and axial velocity distributions [11]. Close to the tube discharge end, the radial and axial gas velocities exceed considerably the liquid velocities because of the large pressure differential between the tube exit and the ambient atmosphere which produces an expansion of the gas but not

that of the liquid. The liquid can, therefore, be only dragged along with the gas and its velocity can increase until it reaches the velocity of the gas. Because the inertia of the liquid phase is larger than that of the gas phase, the former phase has the tendency to remain close to the jet axis and the predicted void fraction distribution in the jet is in accord with this explanation as well as with the X-ray measurements [17]. Further comparisons of the numerical results of flow distribution in the jet between the saturated and subcooled liquid conditions in the vessel reveal that the subcooled liquid has a greater tendency to disperse radially which may be explained by the degree of hydrodynamic and thermal nonequilibrium in the flow. As noted above, the subcooled liquid exiting from a tube has a greater degree of nonequilibrium than the saturated liquid and this, in turn, affects the distribution of phases in the two-phase jet expansion region.

4. SUMMARY AND CONCLUSIONS

Two-phase flow nonequilibrium models of the critical flow in tubes and in the jet expansion region were presented and used to study the flow distribution. The model predictions were sucessfully compared with the steam-water experimental data of subcooled and saturated liquid discharging from a vessel at different stagnation pressures through variable length pipes into an ambient air atmoshpere. The results show that the subcooled liquid discharge through short tubes produces considerable hydrodynamic and thermal nonequilibrium at the tube exit and that the exit flow conditions are responsible for producing a large degree of nonequilibrium in the two-phase flow expansion region. Because of this, the total pressure distribution in the jet exhibits considerable axial and radial dispersion. The radial pressure distribution is shown to exibit a double peak and has a greater dispersion for the subcooled liquid discharge. The liquid phase has a tendency to remain close to the jet axis and the gas to disperse in the radial direction.

5. REFERENCES

[1] G.B. Wallis, Critical Two-Phase Flow, Int. J. Multiphase Flow 6 (1980) 97-112.

[2] P. Saha, A Review of Two-Phase Steam-Water Critical Flow Models with Emphasis on Thermal Nonequilibrium, Brookhaven National Laboratory Report, BNL-NUREG-50907 (1978).

[3] H.S. Isbin, Some Observations on the Status of Two-Phase Critical Flow Models, Int. J. Multiphase Flow 6 (1980) 131-138.

[4] H.J. Richter, Separated Two-Phase Flow Model: Application to Critical Two-Phase Flow, Int. J. Multiphase Flow 9 (1983) 511-530.

[5] F. Dobran, Discharge of Two-Phase Critical Flow Through Tubes, Stevens Institute of Technology Report, ME-RT-84016 (December 1984).

[6] G.B. Wallis, One-Dimensional Two-Phase Flow (McGraw Hill, New York, 1969).

[7] C.W. Solbrig, J.H. McFadden, R.W. Lyczkowski and E.D. Hughes, Heat Transfer and Friction Correlations Required to Describe Steam Water Behavior in Nuclear Safety Studies, AIChE Symp. Series 174 (1978) 100-128.

[8] D. Chisholm, Pressure Gradients Due to Friction During the Flow of Evaporating Two-Phase Mixtures in Smooth Tubes and Channels, Int. J. Heat Mass Transfer 16 (1973) 347-348.

[9] M.D. Alamgir and J.H. Lienhard, Correlations and Pressure Undershoot During Hot-Water Depressurization, J. Heat Transfer 103 (1981) 52-55.

[10] J.A. Boure, A.A. Fritte, M.M. Giot and M.L. Reocreux, Highlight of Two-Phase Critical Flow, Int. J. Multiphase Flow 3 (1976) 1-22.

[11] F. Dobran, Analysis and Computation of Two-Phase Flow Jets with Phase Change, Stevens Institute of Technology Report, ME-RT-85010 (April 1985).

[12] F. Dobran, A Two-Phase Fluid Model Based on the Linearized Constitutive Equations, in Advances in Two-Phase Flow and Heat Transfer, Vol. I, ed. S. Kakac and M. Ishii (Martinus Nijhoff Publ., Netherlands, 1983) pp.41-59.

[13] F. Dobran, Constitutive Equations for Multiphase Mixtures of Fluids, Int. J. Multiphase Flow 10 (1984) 273-305.

[14] L. Lapidus and G.F. Pinder, Numerical Solution of Partial Differential Equations in Science and Engineering (Wiley, New York, 1982).

[15] F. Dobran, A Non Equilibrium Model for the Analysis of Two-Phase Critical Flows in Tubes, Proc. Symp. on Multiphase Flow and Heat Transfer, ASME, New York, 1985, to appear.

[16] G.P. Celata, M. Cumo, G.E. Farello and P.C. Incalcaterra, Physical Insight in the Evaluation of Jet Forces in LOCA, 5th Int. Meeting on Thermal Hydraulics in Reactor Safety, Kalshrushe, Germany, September 1984.

[17] G.P.Celata, M. Cumo and G.F. Farello, X-Ray Analysis in Unbounded Two-Phase Critical Flows, Specialists Meeting on Small Break LOCA Analysis in LWR's, Pisa, Italy, 23-27 June 1985.

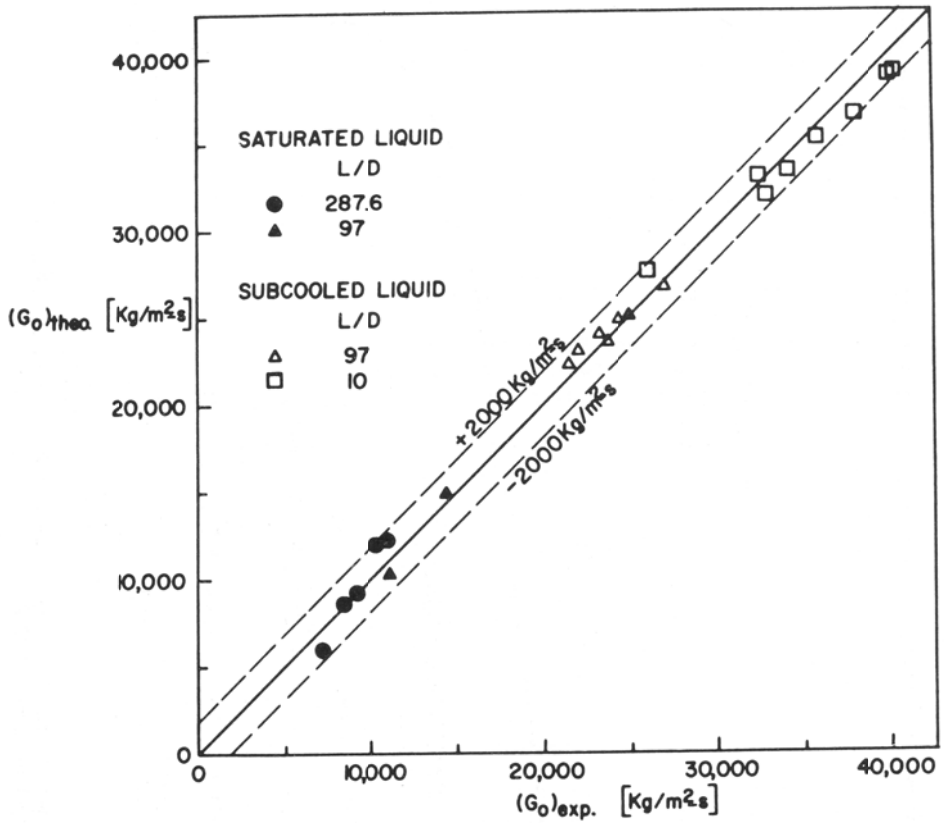

Fig. 1 Comparison of the Predicted Critical Flow Rates with the Experimental Data of Subcooled and Saturated Liquid

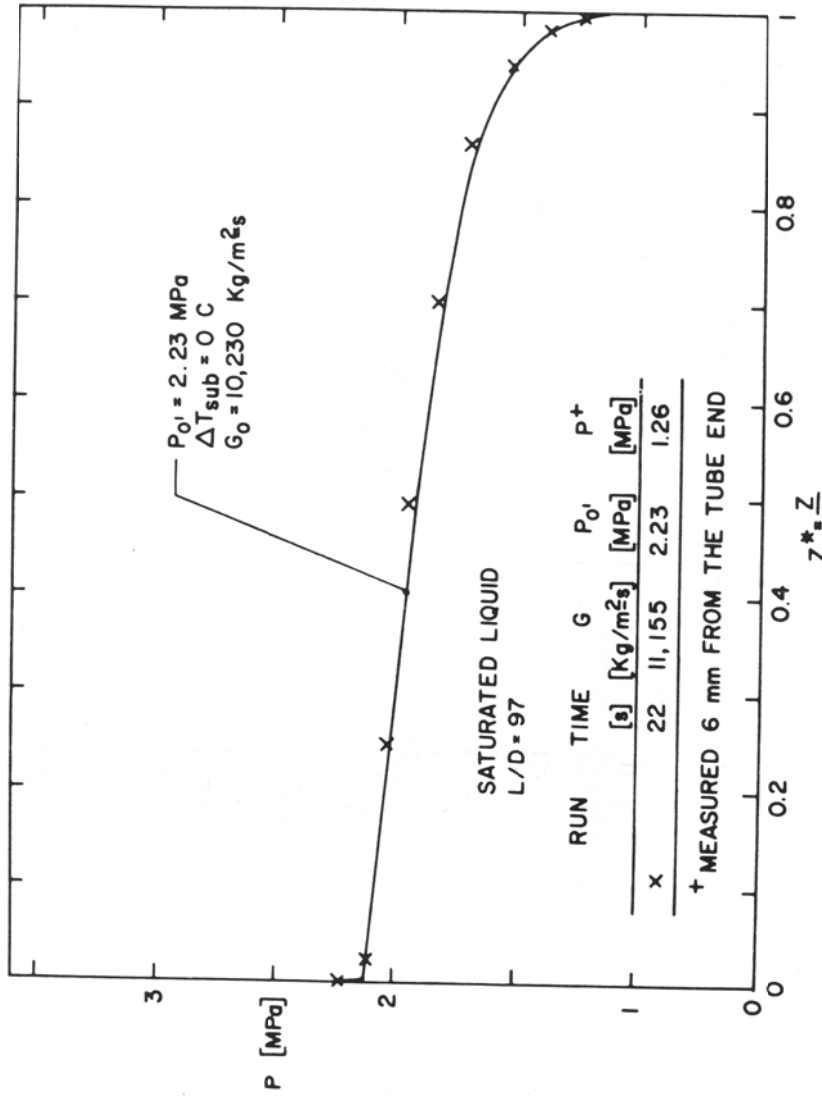

Fig. 2 Comparison of the Predicted Pressure Distribution Along the Tube with the Experimental Data

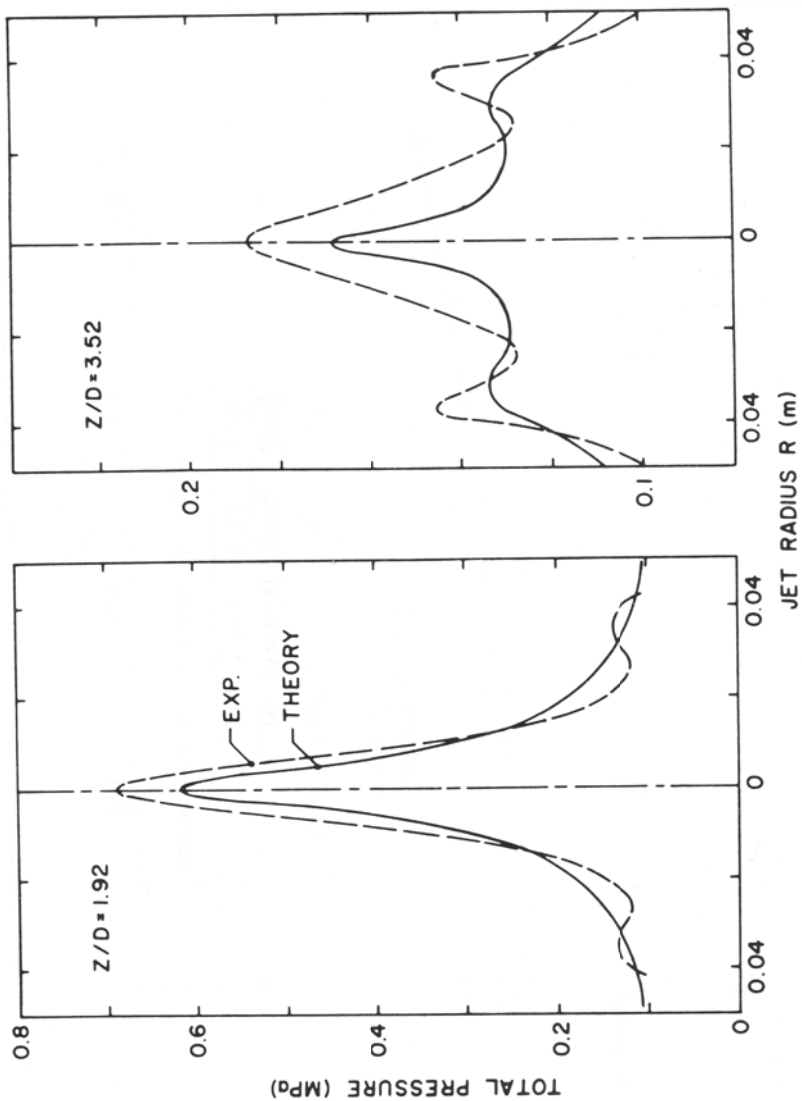

Fig. 3 Comparison of the Predicted Pressure Distribution in the Jet with the Experimental Data of Saturated Liquid

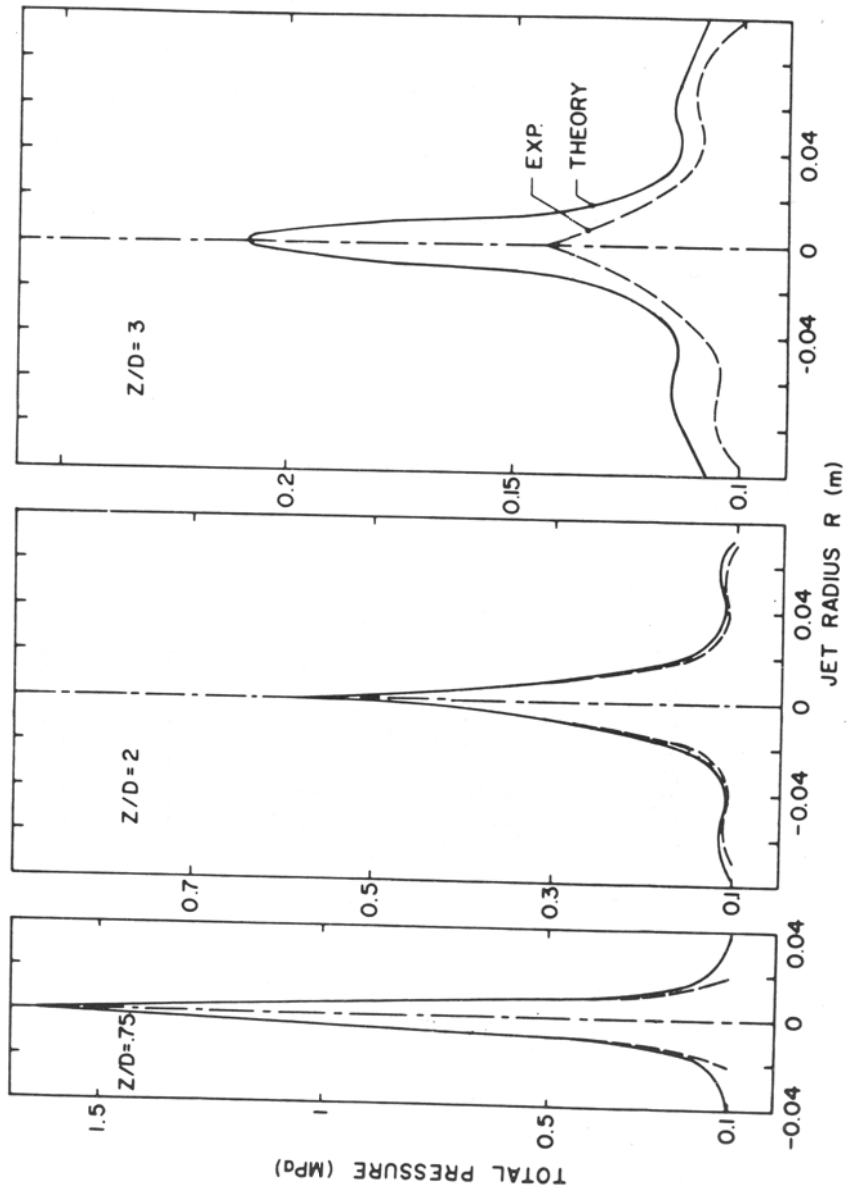

Fig. 4 Comparison of the Predicted Pressure Distribution in the Jet with the Experimental Data of Subcooled Liquid